THE JOURNAL OF PHYSICAL CHEMISTRY A

pubs.acs.org/JPCA Article

Understanding Trends in Molecular Bond Angles

Published as part of The Journal of Physical Chemistry virtual special issue "Paul Geerlings Festschrift".

Gerrit-Jan Linker,* Piet Th. van Duijnen, and Ria Broer

Cite This: *J. Phys. Chem. A* 2020, 124, 1306−1311 Read Online

ACCESS | Metrics & More | Article Recommendations | Supporting Information

ABSTRACT: Trends in bond angle are identified in a systematic study of more than a thousand symmetric A_2B triatomic molecules. We show that, in series where atoms A and B are each varied within a group, the following trends hold: (1) the $A-B-A$ bond angle decreases for more polarizable central atoms B, and (2) the $A-B-A$ angle increases for more polarizable outer atoms A. The physical underpinning is provided by the extended Debye polarizability model for the chemical bond angle, hence our present findings also serve as validation of this simple classical model. We use experimental bond angles from the literature and, where not available, we optimize molecular geometries with quantum chemical methods, with an open mind with regards to the stability of these molecules. We consider main group elements up to and including the sixth period of the periodic table.

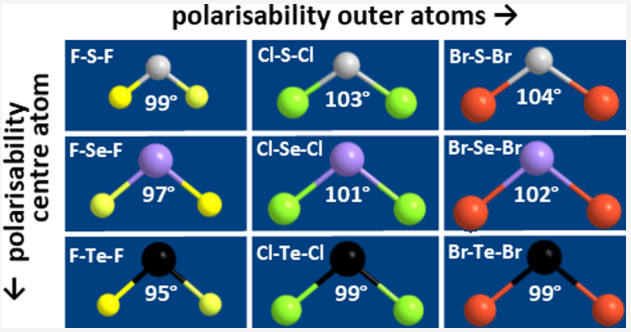

INTRODUCTION

After the chemical bond, the bond angle is the most important structural parameter in chemistry. Nowadays we have a rather good understanding of the variations of the chemical bond from quantum chemical calculations. For the molecular bond angle various models have been proposed. Early qualitative understanding of geometrical configurations of chemical bonds in molecules arose from the analysis of hybridizations of s, p, and d atomic orbitals and were given by Pauling[1] and Slater[2] in 1931. Other guidelines were later given by Mulliken[3,4] and by Walsh.[5−14] From the relation of ionization energies to the bond angle, Mulliken deduced, using a molecular orbital (MO) model, that molecules with 15 or 16 valence electrons have a linear geometry while molecules with 17 to 20 electrons are bent. Walsh explained the molecular geometry of small molecules from the dependence of orbital energies on the bond angle. Sidgwick and Powell[15] considered the geometrical arrangement of bonded and nonbonded (lone) electron-pairs in a molecule. This idea was developed further by Gillespie and Nyholm who rationalized the spatial arrangement of electron pairs around an atom in a molecule in such a way as to minimize their mutual Pauli repulsion in the (extended) Valence Shell Electron Pair Repulsion (VSEPR) model.[16,17] It classifies molecular geometries for main-group elements successfully on this basis with the notable exceptions of alkali metal dihalides[18] (CaX_2, SrX_2, BaX_2) and the dihydrides SrH_2 and BaH_2 for which explanations were sought in terms of d-orbital involvement or nonspherical core distortions.[19−22] It is also possible to look at nonlinear bond angles as distortions from the higher symmetry linear conformation for which the instability is ascribed to the (pseudo) Jahn−Teller effect.[23,24] Models for the molecular bond angle that are based on classical electrostatic theory were also proposed. For example, Donald et al.[25] used electrostatic expressions, originating from the work of Rittner,[26] Hildenbrand[27] and DeKock et al.,[28,29] in so-called polarized-ion models. Among the parameters needed for these models are atomic (or ionic) polarizabilities for which values may be difficult to obtain. In a molecule, atomic polarizabilities are formally not related to the molecular polarizability, and, hence, it is not possible to partition it into atomic parts without arbitrariness.[30] Debye noted in 1929[31] that, in H_2O, due to the existence of the dipole moment, the molecule was either linear with two different H−O distances, or angular. He modeled H_2O with an O^{2-} ion of a finite radius, and two protons, and showed that the nonsymmetrical, linear model was instable against bending. For the symmetric, bent form the protons were allowed to move on the O-radius. He reasoned that induction energy stabilizes an angular geometry. In H_2O, at the polarizable O^{2-} ion, a dipole $\vec{\mu} = \alpha\vec{F}$ is induced in first response to the electric field $\vec{F}$ due to the two protons. The polarization energy, needed to create the dipole at oxygen, is $U_{pol} = +\frac{1}{2}\alpha F^2$. The induced dipole μ is stabilized by the inducing field: $U_d = -\alpha F^2$. The net effect is induction stabilization, that is, a lower internal energy of the molecule:

Received: October 31, 2019
Revised: January 16, 2020
Published: January 27, 2020

https://dx.doi.org/10.1021/acs.jpca.9b10248
J. Phys. Chem. A 2020, 124, 1306−1311

$U_{ind} = U_{pol} + U_d = -\frac{1}{2}\alpha F^2$. The induced dipole is largest at small angles where the resultant electric field is largest; however, at these angles the stabilization is counteracted by the repulsion of the outer atoms.

Some years ago, we extended this model,[32] by introducing polarizabilities on all atoms, and considered all electrostatic interactions between monopoles and induced dipoles at all three atomic centers. Where Debye used fully ionized atoms, we used a charge transfer q. Our model explains the bond angle in terms of the α_A/α_B ratio of the polarizabilities of the free atoms α_A and α_B (for a list of atomic polarizabilities we refer to Table S19 of the Supporting Information). By observing the change of optimum bond angle with the change of the polarizability ratio, two bond angle trends were identified: (1) the bond angle decreases for more polarizable central atoms, and (2) the angle increases for more polarizable outer atoms. This leads to the prediction of bond angle trends with just the information available from the period table of elements. Atomic polarizability within a group increases for atoms from higher periods (rows). Similarly, if the ratio of polarizabilities is changed by, for example, electronic excitation, trends can be explained. When this model is applied to the CO_2 molecule, the rationalization of its linear ground state geometry is that there is too little polarizable electron density around the carbon nucleus to initiate bending through the induction of a dipole at the carbon atom. In the lowest singlet excited states of CO_2, there is substantial charge transfer from oxygen to carbon: about 0.25 electrons. These states[33] have a bond angle of about 120°. When the model is applied to the H_2O molecule, the density of electrons around the oxygen atom that are not involved in bonding and are not core electrons is sufficiently polarizable for a dipole to be induced to stabilize a nonlinear geometry.

In the literature, a number of contributions discuss a similar effect. Reasoning from the principle of chemical softness, von Szentpály[34−36] formulated the hard-bends-soft rule: "hard ligands exert a classical bending force on a soft central atom". In 1985, Andreoni et al.[37] showed that a structural classification of molecules and clusters from valence electron orbital radii is possible, stressing the importance of the central atom. Broader efforts to search for periodic laws for the behavior of small molecules were undertaken by Hefferlin and co-workers, resulting in triatomic periodic systems.[38] Geerlings and co-workers[39] (this paper is part of a festschrift in honor of professor Paul Geerlings) extended the early work of Parr et al.[40] giving sharp definitions for well-known chemical concepts, allowing the calculation of important properties such as electronegativity and electronic polarizability in the framework of density functional theory (DFT). DFT is also known to predict molecular geometries accurately. In this work, however, we choose to use multiconfigurational wave function based methods to obtain the geometries of a large number of triatomic molecules, in order to be able to treat static and dynamic electron correlation separately.

The rationalization and understanding of bond angle trends can have implications, for example, in the field of catalysis. It was shown[41] that for particular catalysts the activation is related to bite-angle strain, which in turn might be related to the ratio of polarizabilities. We suggest that some off-linear metal−ligand bond angles in ruthenium and rhodium complexes can be explained with this model. We anticipate that, with similar reasoning, angles can be understood in asymmetric triatomic molecules (examples by Prasad et al.[42]), in molecules with different electronic excited or charged states, and in weakly bonded systems (examples by Remko[43]). We showed in previous work that also the geometry of ring structures can be rationalized. On the basis of the changes in partial atomic charges we could rationalize that the ionized tetrathiafulvalene molecule is planar while the neutral molecule is off-planar.[32]

In this paper we look for trends in the molecular bond angle in series of symmetric A_2B molecules for which atoms A and B are each varied within one group of the periodic table. We obtained experimental bond angles from the literature and computed angles where they are not available. These trends are compared to trends that follow the extended Debye polarizability model.

COMPUTATIONAL DETAILS

Neutral $A-B-A$ molecules in their lowest spin singlet or doublet electronic state are considered. For most of the molecules we studied, this is the ground state. We selected main group elements from the first six periods of the periodic table with two exceptions: First group elements were excluded as center atoms, and noble gas elements were excluded entirely. We expect the optimum geometry of the molecules to be C_{2v} symmetric[44] but we also explore the possibility of electronic configurations with lower symmetry. We perform the optimizations first on all 1080 molecules with the CASSCF method in which we chose to correlate all s and p valence electrons. Next, the geometries of 225 mainly angular molecules are reoptimized at the CASPT2 level in order to include the effects of both static and dynamic correlation.

The possibility to inadvertently obtain an improper electronic configuration is inherent to the CASSCF/CASPT2 technique. We checked the CASSCF results obtained with C_{2v} symmetry (both for electron density and nuclei) against those obtained with C_1 symmetry. It should be noted when comparing optimized bond angles to experiment, that experimentally, the average angle is usually reported.[45]

We used the MOLCAS software.[46] We mostly made use of the ANO-RCC basis set,[47,48] with static relativistic effects taken care of using a Douglass-Kroll scheme,[49,50] but where possible the ANO-L basis set[51,52] was used instead. Besides static relativistic effects we do not account for other relativistic effects, such as spin−orbit coupling. We did not correct for basis set superposition errors since the basis sets are rather large and we discuss only angular molecules in which there is negligible $A-A$ bonding. The active orbital space contains n s-, and p-valence electrons in n orbitals when the number of s and p valence electrons is less than 12, we use n electrons in 12 orbitals space in other cases. For further computational details we refer to the Supporting Information.

RESULTS

When analyzing bond angles obtained from experiment, we observe trends in series of symmetric A_2B molecules for which A and B are same group atoms (odd numbered Tables S3−S17). Next, we performed CASSCF optimizations. We analyzed the geometry in series of A_2B molecules in which atoms A and B are each varied within one group of the periodic table, for example, the H_2O series is denoted (1−16−1). This way we identified several series of molecules where bond angle trends may be analyzed (Table S1). Next, 225 mainly angular

https://dx.doi.org/10.1021/acs.jpca.9b10248
J. Phys. Chem. A 2020, 124, 1306−1311

Table 1. $A-B-A$ Bond Angles (deg) at the CASPT2 Level (a) and α_A/α_B Ratio of Experimental Free Atom Polarizabilities (Table S19), (b) with Atoms B in Group 16 and Atoms A in Group 1. Atomic Polarizability of Oxygen Is α_O = 5.41 au

a								b						
B	A =	H	Li	Na	K	Rb	Cs	B	A =	H	Li	Na	K	Rb	Cs
O		104	180					O		0.83	30	30	54	59	74
S		92	120		180	180		S		0.23	8.4	8.3	15	16	20
Se		91	116		180	180	180	Se		0.18	6.4	6.4	12	13	16
Te		90	104		138	180	180	Te		0.12	4.4	4.4	7.9	8.6	11
Po		89	96		127	179	180	Po		0.10	3.6	3.5	6.4	7.0	8.7

Table 2. $A-B-A$ Bond Angles (deg) at the CASPT2 Level (a) and α_A/α_B Ratio of Experimental Free Atom Polarizabilities (Table S19) (b) with Atoms B in Group 14 and Atoms A in Group 17. Atomic Polarizability of Carbon Is α_C = 11.9 au

a						b						
B	A =	F	Cl	Br	I	B	A =	F	Cl	Br	I	At
C		105	109	110		C		0.32	1.2	1.7	3.0	3.4
Si		101	103	102	103	Si		0.10	0.41	0.57	0.99	1.1
Ge		97	100	101	102	Ge		0.09	0.36	0.50	0.88	0.99
Sn		96	98	99	101	Sn		0.07	0.28	0.40	0.69	0.78
Pb		95	98	99	100	Pb		0.08	0.32	0.45	0.79	0.88

molecules are reoptimized at the CASPT2 level of theory (Table S2) in order to include both the effects of static and dynamic correlation. Overall, our CASPT2 bond angles compare well with values from experimental and other computational work found in the literature (Figures S1−S6). The CASPT2 bond angles were analyzed within each molecular series (even numbered Tables S4−S18).

Exemplary for the bond angle trends that we identify are those found in the (1−16−1), and in the carbon group dihalides, the (17−14−17) series of molecules (Table 1a, Table 2a). For a given outer atom A, the angle is progressively smaller when the inner atom B is exchanged by a larger, more polarizable element (from a higher period of the periodic table). The second trend we find is that $A-B-A$ bond angles in the series become increasing large when, for a given inner atom, the outer atom is substituted by a larger, more polarizable, atom. For triangular molecules, in which there are both $A-B$ and $A-A$ bonds, bond angles were omitted from the tables. The bond angle is proportional to the α_A/α_B ratio of atomic polarizabilities (Table 1b, Table 2b).

Examples of difficult cases are indium and thallium dihydrides and dihalides, and also some of the pnictogen dichalcogenides. In the (1−13−1) and (17−13−17) molecular series (Table S6), the angles in indium centered molecules are larger than those in corresponding gallium centered molecules. Thallium molecules have larger angles than the corresponding indium centered molecules. In both cases we expected smaller angles. The polarizability of indium is larger than the polarizability of gallium (Table S19). Surprisingly, for thallium the experimental polarizability is considerably smaller than that of indium, which could offer an explanation for the larger angles we found in the thallium centered molecules.

In the pnictogen dichalcogenede (16−15−16) molecular series (Table 3) PO_2 has a somewhat larger bond angle than NO_2 for which we expected a smaller angle. Also NS_2 has a larger angle than NSe_2 for which a smaller angle would fit the second bond angle trend from NO_2 to NSe_2. We note that the angle differences in these cases are of the order of the classical amplitude of the zero point vibration in these molecules (*vide infra*).

Table 3. $A-B-A$ Bond Angles (deg) at the CASPT2 Level with Atoms B in Group 15 and Atoms A in Group 16

B	A =	O	S	Se
N		134	150	147
P		136	132	
As		128		
Sb		123		
Bi		117		

DISCUSSION AND CONCLUSIONS

When three atoms are brought together to form a neutral symmetric A_2B molecule, charge transfer causes atomic electric moments to be induced. Our model shows that these induced moments are important for the bond angle to form. Charge transfer is the largest in cases for which there is a large difference in electronegativity of constituent atoms. In group 1 centered molecules this is most extreme. Many of them are unstable in the sense they can be considered as A_2 molecules with a coordinated B atom. In other cases there are both $A-B$ and $A-A$ bonds in the molecule, giving rise to a triangular molecular geometry. Hence, group 1 centered molecules are not discussed.

In group 2 dihalides, we can consider the molecules as B^{2+} with two A^- ions. In these cases, the polarizability of the center B atom is largely reduced while that of the A atoms is enhanced, when compared to the polarizabilities of the free atoms. For example, in MgF_2, the polarizability of Mg^{2+} is likely much smaller than that of the neutral free Mg atom, due to its empty valence shell. And the polarizability of the F^- ions will be larger than in the free F atom, due to its full valence shell. Owing to the small remaining polarizability of the center atom and the enhancement of it in the halogen outer atoms, these molecules are linear: magnesium (and also beryllium) dihalides are linear. In Table 4 section a, the bond angles in the alkali earth centered difluorides are presented. The polarizabilities and polarizability ratios of the constituent atoms are presented in Table 4 sections b and c, respectively, The polarizability of calcium is more than double that of magnesium. Calcium centered dihalides are quasi-linear. The yet larger alkali earth

https://dx.doi.org/10.1021/acs.jpca.9b10248
J. Phys. Chem. A 2020, 124, 1306−1311

Table 4. $A-B-A$ Bond Angles at the CASPT2 Level (a) for Alkali Earth Centered Difluorides; Relevant Atomic Polarizabilities (Table S19a) (b), and α_A/α_B Polarizability Ratios (c)

a		b		c	
B	A = F	atom	polarizability (au)	B	A = F
Be	180	F	3.76	Be	0.10
Mg	180	Be	37.8	Mg	0.05
Ca	180	Mg	71.5	Ca	0.02
Sr	142	Ca	154	Sr	0.02
Ba	130	Sr	186	Ba	0.01
		Ba	268		

metals, Sr and Ba, have a much larger polarizability than calcium. This is likely due to the polarizability of the many electrons in full outer-core shells. Strontium and barium centered dihalide molecules are angular.

In the other series of molecules we observe angular molecular geometries in which there is an intermediate electron transfer. In these cases, bond angles follow bond angle trends that are predicted by the extended Debye polarizability model for the chemical bond angle,[32] implying that our present findings serve as a further validation of this model. It also shows that a qualitative understanding of bond angle trends is possible by just using classical electrostatics. A rationalization of bond angle trends is possible in neutral symmetric triatomic molecules without performing computations, just using the information about atomic polarizabilities from the periodic table. When excess or lack of electrons is located on the center atom in anions and cations, respectively, we anticipate that bond angles in anions are smaller in general, and in cations they are larger, compared to the neutral molecule. By the same reasoning excited states may have a sharper angle when charge is transferred from the outer atoms to the central atom, as for example occurs in the lowest excited states of CO_2.

In summary, we identified bond angle trends by looking into experimental bond angles and where they are not available by optimizing the geometries of symmetric A_2B molecules at the full valence CASSCF/CASPT2 level for the main group elements up to the sixth period. The dominant bond angle trend we identified is connected to the inverse relation between the molecular angle and the polarizability volume of the central atom B. The molecular angle becomes smaller when, for a given atom A, in a series of A_2B molecules, atom B is taken from the same group but from a higher period of the periodic table. The angle becomes larger in a series of A_2B molecules if, for a given atom B, a more polarizable atom A (from a higher period) is taken. This is the second bond angle trend we found. Difficult cases include the angular thallium and indium centered A_2B molecules. They have a larger angle than we expected from their low position in the periodic table because, generally, the atomic polarizability is larger for same group elements in higher periods. We pointed out that the experimental polarizability of thallium is smaller than that in indium, which offers an explanation for our results. According to Fleig,[53] relativistic effects in group 13 atoms decrease the polarizability. Relativistic effects are negligible for the light elements B and Al, become significant for Ga and In, and are large for Tl. We found no experimental angles for thallium or indium dihydrides and dichalcogenides. We reported bond angles at potential energy minima and it should be noted that the zero-point vibrations also change the bond angle and these bond angle changes are rather different for different molecules. To give an indication for a few relevant molecules, we estimate the classical amplitude of the bending mode at the CASPT2 level of theory. The amplitudes are ±13° for H_2O, around ±6° for NO_2, NS_2, NSe_2, and PO_2, around ±4° for O_3, S_3, and SO_2, and ±11° for InH_2 and TlH_2. Compared to optimal angles obtained at the CASSCF level, the effect of the inclusion of dynamical correlation through CASPT2 is negligible for small molecules. However, for some larger molecules the effect is significant. For example, in barium dihalides some CASPT2 bond angles are 10° smaller compared to the CASSCF angle. In our experience, the polarizability of the electron density is often not described sufficiently accurate at levels of theory in which little dynamic electron correlation is recovered. From our bond angle model it follows that a poor description of the polarizability around an atom causes a too large angle. For the chalcogen centered (2−16−2) molecules $Mg_2S...Ba_2Po$ the inclusion of a dynamical correlation has a profound effect on the molecular geometry. These molecules are angular at the CASSCF level, but at the CASPT2 level of theory these molecules adopt a triangular optimum conformation.

■ ASSOCIATED CONTENT

Supporting Information

The Supporting Information is available free of charge at https://pubs.acs.org/doi/10.1021/acs.jpca.9b10248.

Details of CASSCF/CASPT2 calculations as well as representative angles found in the literature; results analyzed in tables and graphs for groups of molecules in which we identified the bond angle trends; list of atomic polarizabilities (PDF)

■ AUTHOR INFORMATION

Corresponding Author

Gerrit-Jan Linker − *Zernike Institute for Advanced Materials, University of Groningen, 9712 CP Groningen, The Netherlands; MESA+ Institute for Nanotechnology, University of Twente, 7522 NB Enschede, The Netherlands;* orcid.org/0000-0001-9416-3588; Email: g.linker@utwente.com

Authors

Piet Th. van Duijnen − *Stichting Moleculaire Quantum Mechanica, 9351 SB Leek, The Netherlands*

Ria Broer − *Zernike Institute for Advanced Materials, University of Groningen, 9712 CP Groningen, The Netherlands;* orcid.org/0000-0002-5437-9509

Complete contact information is available at: https://pubs.acs.org/10.1021/acs.jpca.9b10248

Notes

The authors declare no competing financial interest.

■ REFERENCES

(1) Pauling, L. The nature of the chemical bond. Application of results obtained from the quantum mechanics and from a theory of paramagnetic susceptibility to the structure of molecules. *J. Am. Chem. Soc.* **1931**, *53*, 1367.

(2) Slater, J. C. Directed valence in polyatomic molecules. *Phys. Rev.* **1931**, *37*, 481.

(3) Mulliken, R. S. Electronic structures and spectra of triatomic oxide molecules. *Rev. Mod. Phys.* **1942**, *14*, 204.

(4) Mulliken, R. S. Chemical bonding. *Annu. Rev. Phys. Chem.* **1978**, *29*, 1.
(5) Walsh, A. D. The electronic orbitals, shapes, and spectra of polyatomic molecules. part I. AH_2 molecules. *J. Chem. Soc.* **1953**, *466*, 2260.
(6) Walsh, A. D. The electronic orbitals, shapes, and spectra of polyatomic molecules. part II. Non-hydride AB_2 and BAC molecules. *J. Chem. Soc.* **1953**, *467*, 2266.
(7) Walsh, A. D. The electronic orbitals, shapes, and spectra of polyatomic molecules. part III. HAB and HAAH molecules. *J. Chem. Soc.* **1953**, *468*, 2288.
(8) Walsh, A. D. The electronic orbitals, shapes, and spectra of polyatomic molecules. part IV. Tetratomic hydride molecues, AH_3. *J. Chem. Soc.* **1953**, *469*, 2296.
(9) Walsh, A. D. The electronic orbitals, shapes, and spectra of polyatomic molecules. part V.Tetratomic, nonhydride molecules, AB_3. *J. Chem. Soc.* **1953**, *470*, 2301.
(10) Walsh, A. D. The electronic orbitals, shapes, and spectra of polyatomic molecules. part VI. H_2AB molecules. *J. Chem. Soc.* **1953**, *471*, 2306.
(11) Walsh, A. D. The electronic orbitals, shapes, and spectra of polyatomic molecules. part VII. A note on the near-ultra-violet spectrum of acetaldehyde. *J. Chem. Soc.* **1953**, *472*, 2318.
(12) Walsh, A. D. The electronic orbitals, shapes, and spectra of polyatomic molecules. part VIII. Pentatomic molecules: CH_3I. *J. Chem. Soc.* **1953**, *473*, 2321.
(13) Walsh, A. D. The electronic orbitals, shapes, and spectra of polyatomic molecules. part IX. Hexatomic molecules: ethylene. *J. Chem. Soc.* **1953**, *474*, 2325.
(14) Walsh, A. D. The electronic orbitals, shapes, and spectra of polyatomic molecules. part X. A note on the spectrum of benzene. *J. Chem. Soc.* **1953**, *475*, 2330.
(15) Sidgwick, N. V.; Powell, H. M. Stereochemical types and valency groups. *Proc. R. Soc.* **1940**, *A176*, 153.
(16) Gillespie, R. J. The electron-pair repulsion model for molecular geometry. *J. Chem. Educ.* **1970**, *47* (1), 18.
(17) Bytheway, I.; Gillespie, R. J.; Tang, T.-H.; Bader, R. F. W. Core distortions and geometries of the difluorides and dihydrides of Ca, Sr, and Ba. *Inorg. Chem.* **1995**, *34*, 2407.
(18) Hargittai, M. Molecular structure of metal halides. *Chem. Rev.* **2000**, *100*, 2233.
(19) Kaupp, M. Non-VSEPR" structures and bonding in d^0 Systems. *Angew. Chem., Int. Ed.* **2001**, *40*, 3534.
(20) Kaupp, M.; Schleyer, P. v. R.; Stoll, H.; Preuss, H. The question of bending of the alkeline earth dihalides MX_2 (M = Be, Mg, Ca, Sr, Ba; X = F, Cl, Br, I). An ab Initio pseudopotential study. *J. Am. Chem. Soc.* **1991**, *113*, 6012.
(21) Gillespie, R. J. Chem. The VSEPR model revisited. *Chem. Soc. Rev.* **1992**, *21*, 59.
(22) Gillespie, R. J.; Bytheway, I.; Tang, T.-H.; Bader, R. F. W. Geometry of the fluorides, oxofluorides, hydrides, and methanides of vanadium(V), chromium(VI), and molybdenum(VI): Understanding the geometry of non-VSEPR molecules in terms of core distortion. *Inorg. Chem.* **1996**, *35*, 3954.
(23) Rocha, C. M. R.; Varandas, A. J. C. The Jahn-Teller plus pseudo-Jahn-Teller vibronic problem in the C_3 radical and its topological implications. *J. Chem. Phys.* **2016**, *144*, No. 064309.
(24) Bersuker, I. B. Pseudo-Jahn−Teller Effect: A two-state paradigm in formation, deformation, and transformation of molecular systems and solids. *Chem. Rev.* **2013**, *113*, 1351.
(25) Donald, K.; Mulder, W.; Szentpály, L. J. Success and failure of polarized-ion models: Bending and atomization energy of groups 2 and 12 dihalides. *J. Chem. Phys.* **2003**, *119*, 5423.
(26) Rittner, E. S. Binding energy and dipole moment of alkali halide molecules. *J. Chem. Phys.* **1951**, *19*, 1030.
(27) Hildenbrand, D. L. Model calculations of the thermochemical properties of gaseous metal halides. *J. Electrochem. Soc.* **1979**, *126*, 1396.
(28) DeKock, R. L.; Peterson, M. A.; Timmer, L. K.; Baerends, E. J.; Vernooijs, P. A theoretical study of the linear versus bent geometry for several MX_2 molecules: MgF_2, CaH_2, CaF_2, CeO_2 and $YbCl_2$. *Polyhedron* **1990**, *9*, 1919.
(29) DeKock, R. L.; Peterson, M. A.; Timmer, L. K.; Baerends, E. J.; Vernooijs, P. *Polyhedron Erratum* **1991**, *10*, 1965.
(30) Rick, S. W.; Stuart, S. J. Potentials and algorithms for incorporating polarizability in computer simulations. *Rev. Comput. Chem.* **2002**, *18*, 89.
(31) Debye, P. *Polar Molecules*; Dover, 1929.
(32) Linker, G. J.; van Duijnen, P.Th.; van Loosdrecht, P. H. M.; Broer, R. Off-planar geometry and structural instability of EDO-TTF explained by using the extended Debye polarizability model for bond angles. *J. Phys. Chem. A* **2012**, *116*, 7219.
(33) Wiberg, K. B.; Wang, Y.; de Oliveira, A. E.; Perera, S. A.; Vaccaro, P. H. Comparison of CIS- and EOM-CCSD-Calculated Adiabatic excited-state structures. Changes in charge density on going to adiabatic excited states. *J. Phys. Chem. A* **2005**, *109*, 466.
(34) von Szentpály, L.; Schwerdtfeger, P. Which double-octet ABC molecules are bent? CI calculations on CaF_2 and a softness criterion to predict bending. *Chem. Phys. Lett.* **1990**, *170* (5, 6), 555.
(35) von Szentpály, L. J. Hard bends soft: Bond angle and bending force constant predictions for dihalides, dihydrides, and dilithides of groups 2 and 12. *J. Phys. Chem. A* **2002**, *106*, 11945.
(36) Prasad, S.; Wittmaack, B. K.; Donald, K. J. Bending ternary dihalides. *J. Phys. Chem. A* **2018**, *122* (46), 9065.
(37) Andreoni, W.; Galli, G.; Tosi, M. Structural classification of AB_2 molecules and A_3 clusters from valence electron orbital radii. *Phys. Rev. Lett.* **1985**, *55* (17), 1734.
(38) Barrow, J.; Caviness, K.; Hefferlin, R.; Nash, D. Periodic trends in constants of triatomic molecules. *Int. J. Quantum Chem.* **2016**, *116*, 1072.
(39) Geerlings, P.; De Proft, F.; Langenaeker, W. Conceptual density functional theory. *Chem. Rev.* **2003**, *103* (5), 1793.
(40) Parr, R. G.; Yang, W. Density-functional theory of the electronic structure of molecules. *Annu. Rev. Phys. Chem.* **1995**, *46*, 701.
(41) Wolters, L. P.; van Zeist, W.-J.; BickelHaupt, F. M. New concepts for designing d^{10}-$M(L)_n$ catalysts:d regime, s regime and intrinsic bite-angle flexibility. *Chem. - Eur. J.* **2014**, *20*, 11370.
(42) Prasad, S.; Wittmaack, B. K.; Donald, K. J. Bending ternary dihalides. *J. Phys. Chem. A* **2018**, *122* (46), 9065.
(43) Remko, M. Structure and gas phase stability of complexes L···M, where M = Li^+, Na^+, Mg^{2+} and L is formaldehyde, formic acid, formate anion, formamide and their sila derivatives. *Chem. Phys. Lett.* **1997**, *270*, 369.
(44) Stanton, J. F. Note: Is it symmetric or not? *J. Chem. Phys.* **2013**, *139*, 46102.
(45) Groner, P. In *Vibrational Spectra and Structure*; Durig, J. R., Ed.; Elsevier: Amsterdam, 2000; Vol. *24*, p 165.
(46) Karlström, G.; Lindh, R.; Malmqvist, P.; Roos, B. O.; Ryde, U.; Veryazov, V.; Widmark, P.; Cossi, M.; Schimmelpfennig, B.; Neogrady, P.; et al. MOLCAS: a program package for computational chemistry. *Comput. Mater. Sci.* **2003**, *28*, 222.
(47) Roos, B. O.; Veryazov, V.; Widmark, P.-O. Relativistic atomic natural orbital type basis sets for the alkaline and alkaline-earth atoms applied to the ground-state potentials for the corresponding dimers. *Theor. Chem. Acc.* **2004**, *111*, 345.
(48) Roos, B. O.; Lindh, R.; Malmqvist, P.-Å.; Veryazov, V.; Widmark, P.-O. Main group atoms and dimers studied with a new relativistic ANO basis set. *J. Phys. Chem. A* **2004**, *108*, 2851.
(49) Douglas, N.; Kroll, N. M. Quantum electrodynamical corrections to the fine structure of helium. *Ann. Phys.* **1974**, *82*, 89.
(50) Hess, B. A. Relativistic electronic-structure calculations employing a two-component no-pair formalism with external-field projection operators. *Phys. Rev. A: At., Mol., Opt. Phys.* **1986**, *33*, 3742.
(51) Widmark, P.-O.; Malmqvist, P.-Å.; Roos, B. O. Density matrix averaged atomic natural orbital (ANO) basis sets for correlated

https://dx.doi.org/10.1021/acs.jpca.9b10248
J. Phys. Chem. A 2020, 124, 1306−1311

molecular wave functions. I: first row atoms. *Theor. Chim. Acta* **1990**, *77*, 291.
(52) Widmark, P.-O.; Persson, B. J.; Roos, B. O. Density matrix averaged atomic natural orbital (ANO) basis sets for correlated molecular wave functions. II: second row atoms. *Theor. Chim. Acta* **1991**, *79*, 419.
(53) Fleig, T. Spin-orbit-resolved polarizabilities of group-13 atoms: four-component relativistic configuration interaction and coupled cluster calculations. *Phys. Rev. A: At., Mol., Opt. Phys.* **2005**, *72*, No. 052506.

https://dx.doi.org/10.1021/acs.jpca.9b10248
J. Phys. Chem. A 2020, 124, 1306−1311